



17 **Abstract**

18 Ponds play a critical role in biogeochemical carbon cycling and have been identified as hot
19 spots of methane (CH₄) emission. Yet, most existing studies focused on ponds in the boreal
20 zone and current estimates of the relevance of ponds in global CH₄ budgets as well as
21 knowledge of the environmental factors regulating their emissions are poorly constrained. Both
22 nutrient concentration and temperature can potentially alter CH₄ dynamics in shallow ponds,
23 but there are still few investigations into the response of CH₄ emission to nutrient enrichment
24 and rising temperatures. Here we studied the magnitude and regulation of two CH₄ pathways
25 (diffusion and ebullition) from a shallow and eutrophic pond located in the subtropical zone in
26 Central China. Ebullitive fluxes were on average 96.4 mg CH₄·m⁻²·d⁻¹ and contributed 88.6%
27 to the total (diffusive + ebullition) CH₄ emissions. Daily CH₄ fluxes were related to daily mean
28 water temperature, with ebullition having a stronger temperature dependence than diffusion
29 (Q_{10} of 5.52 vs. 2.05). Relationships between temperature and CH₄ emission were affected by
30 seasonal variation of the concentration of total phosphorus. The temperature dependence of
31 both ebullitive and diffusive fluxes increased with increasing phosphorous concentration. Our
32 study highlights that increasing eutrophication by anthropogenic impacts and climate warming
33 will increase CH₄ emissions from ponds, thus representing a positive feedback mechanism to
34 global warming.

35

36 Keywords: Subtropical pond; eutrophication; Diel pattern; Temperature dependence; CH₄
37 ebullition;

38



39 **1. Introduction**

40 Methane (CH₄) is an important climate forcing as well as a sensitive indicator of climate
41 change due to its increasing atmospheric concentration and its strong global warming
42 potential, which is 28–36 times higher compared to CO₂ (Houghton et al., 2001; Loulergue
43 et al., 2008). Recent estimates report a 150% increase of atmospheric CH₄ concentration since
44 1750, which is unprecedented over the last 800,000 years (IPCC, 2014). Therefore, a better
45 understanding of CH₄ sources and sinks is urgently needed.

46 Freshwater ecosystems are important for the biogeochemical processes involved in the
47 cycling of CH₄ (Kirschke et al., 2013; Davidson et al., 2015). There is increasing evidence
48 that freshwaters are a globally significant source of CH₄ (e.g. Lundin et al., 2013). But global
49 CH₄ estimates of freshwaters are based on upscaling of few measurements and still highly
50 uncertain (Rasilo et al., 2015). And before that, numerous ponds and lakes were often
51 considered as minor emitters and their importance was neglected compared to wetland
52 emissions (Wik et al., 2016b). Even small ponds were excluded from most estimates of global
53 carbon budgets (Hanson et al., 2007). However, existing observations of CH₄ fluxes from
54 lakes and ponds suggest that they are emission hot spots (Bastviken et al., 2011; Natchimuthu
55 et al., 2014; Wik et al., 2016a). Especially the small ponds, comprising the majority of lentic
56 aquatic systems (Downing et al., 2006), tend to have higher dissolved CH₄ concentration than
57 larger lakes (Downing et al., 2008; Holgerson, 2015). Holgerson and Raymond (2016) found
58 that very small ponds accounted for 40.6% of diffusive CH₄ emissions from lakes and ponds
59 globally, due to their shallow depth, high sediment to water volume ratios, and frequent
60 mixing. Wik et al. (2016a) compared CH₄ emissions from water bodies north of 50°N, and



61 found that small ponds are an important source of CH₄ in northern latitudes. Nevertheless,
62 current data on the abundance, size, and rate of carbon emissions of small ponds are scarce,
63 which may lead to considerable bias at the regional and global scale (Hanson et al., 2007).
64 More research on the cycling of the CH₄ in ponds will be beneficial to more accurately quantify
65 carbon fluxes from inland waters (Holgerson and Raymond, 2016).

66 Several studies have explored the dynamics of CH₄ concentrations and fluxes and have
67 linked them to the pond depth and size, weather variables, organic carbon loading and
68 nutrient status (Hamilton and Kelly, 1994; Kankaala et al., 2013; Xiao et al., 2014;
69 Natchimuthu et al., 2014; Holgerson, 2015; Burger et al., 2016). Yet, some studies often relied
70 on short term (30 min) measurements at monthly intervals and temporal variability was poorly
71 resolved (Peixoto et al., 2015). There is still a lack of robust relationships between pond CH₄
72 and its potential drivers that could facilitate temporal prediction and spatial extrapolation. In
73 addition, most of the studies on CH₄ fluxes from ponds are from the boreal zone, which limits
74 our understanding of inland water carbon cycling at larger scales.

75 CH₄ can be emitted from aquatic systems through different pathways, including ebullition
76 (bubble emission from sediments) and diffusion (gas exchange at the air-water interface).
77 Small and shallow ponds are expected to become hot spots of ebullition due to limited
78 stratification, sediment temperature being strongly related to atmospheric temperature, and
79 direct solar warming of the sediments (Aben et al., 2017). However, most studies focused on
80 diffusive fluxes and neglected the large emission component of ebullition (Aben et al., 2017).
81 In fact, eutrophic ponds have greater potential for CH₄ ebullition because they accumulate
82 more organic carbon (Downing et al., 2008; Anderson et al., 2014). Increasing eutrophication



83 of aquatic ecosystems by human activities may eventually promote CH₄ ebullition, and the
84 strongest increase in ebullition can be expected in shallow water bodies (West et al., 2016;
85 Aben et al., 2017).

86 In addition, carbon dynamics in small ponds may be more sensitive to seasonal variation,
87 such as temperature change (Holgerson, 2015). The proportion of ebullitive and diffusive
88 fluxes to total CH₄ emissions may be disproportionally affected by changes in temperature
89 and the temperature dependence of CH₄ fluxes is different with different degrees of aquatic
90 eutrophication (DelSontro et al., 2016). However, there is still no corresponding model basis
91 to evaluate how the magnitude and relative contributions of CH₄ ebullition and diffusion may
92 respond to climatic and environmental changes, including global warming and cultural
93 eutrophication.

94 This study analyzes CH₄ emissions from a subtropical, shallow and small eutrophic pond in
95 Central China, measured with floating chambers at high temporal resolution (diel variations).
96 We aim at: 1) quantifying CH₄ emissions including diffusive flux and ebullition, with a
97 particular focus on ebullition and its contribution to total CH₄ fluxes; 2) identifying their main
98 influencing factors; and 3) assessing the temperature dependence of ebullitive and diffusive
99 fluxes with different degrees of aquatic eutrophication.

100 **2. Materials and methods**

101 2.1 Study area and monitoring sites

102 The study was conducted in a small and shallow pond, which is located on the campus of
103 China Three Gorges University, Yichang city, Hubei province, Central China (111°18'23"E,
104 30°43'24"N). The region is under a subtropical continental monsoon climate regime. The



105 average depth of the pond is 1.2 m, and its area is approximately 4000 m². The pond bottom
106 was solidified with concrete in 2002-2003 and is now covered with about 20 cm of soft
107 sediments. The main sources of water are natural rainfall and drainage water from streets.
108 Twelve monthly field campaigns, resolving diurnal variations respectively, were conducted
109 between 19 January and 29 December, 2016. All measurements were done at the same sampling
110 site, which was located 0.5 m away from the bank where water depth was ~0.7 m.

111 2.2 In situ CH₄ flux measurement

112 CH₄ flux was measured using a static floating chamber and followed the methods described
113 in Xiao et al. (2014). The chamber was made of a non-transparent, thermally insulated vertical
114 tube with a volume of 43.30 L and a surface area of 0.096 m² (diameter and height are 0.35 and
115 0.45 m respectively). Two fans (12 V, 0.22 A) were fixed in the upper part of the chamber to
116 properly mix the air in the chamber headspace while not disturbing the water surface. The
117 chamber was connected to a CH₄ Analyzer (G2301, Picarro, USA), which was used to monitor
118 the CH₄ concentrations inside the chamber continuously at a frequency of 1 Hz. One buoy was
119 fixed at the lower portion of the chamber, allowing for precise adjustment of the penetration
120 depth of the chamber edge into the water. We used 5 cm penetration depth and only the
121 headspace volume above the water surface was taken into account when calculating the gas
122 flux.

123 Each field campaign was conducted for 24 hours. A single flux measurement was usually
124 finished within 20 minutes and 48 consecutive measurements were conducted during each field
125 campaign. When there was no or little ebullition, CH₄ concentration in the chamber headspace
126 increased nearly linearly over time and single linear regression was used to estimate the



127 diffusive flux of CH₄ (D_{CH_4} , mg CH₄·m⁻²·h⁻¹) (Lambert and Fréchet, 2005). When gas bubbles
128 occurred, the gas concentration in the chamber increased abruptly. Under this situation, the
129 flux due to bubble emission (CH₄ ebullition, B_{CH_4} , mg CH₄·m⁻²·h⁻¹) was estimated using the
130 method described in detail by Xiao et al. (2014). Bubbles were not observed in all 48 chamber
131 deployments during the daily campaigns. Thus, the frequency of daily CH₄ bubbling (F_{BCH_4})
132 was estimated as:

$$133 \quad F_{BCH_4} = \frac{\text{Deployments with Bubbles}}{48} \times 100\% \quad (\text{Eq.1})$$

134 The daily total CH₄ flux (T_{CH_4} , mg CH₄·m⁻²·d⁻¹) was the sum of daily total D_{CH_4} and daily
135 total B_{CH_4} .

136 2.3 Model approach

137 To describe the temperature dependence of CH₄ fluxes, we used a modified Arrhenius
138 equation (Aben et al., 2017):

$$139 \quad F_{CH_4} = F_{20} \times e^{b \times (T - 20)} \quad (\text{Eq.2})$$

140 F_{CH_4} is the CH₄ flux at temperature T (°C); F_{20} and b are the empirical coefficients; F_{20} is the
141 CH₄ flux at 20 °C. This model can be reorganized as a Q_{10} relationship with b :

$$142 \quad b = (\ln Q_{10}) / 10 \quad (\text{Eq.3})$$

143 Q_{10} corresponds to the proportional change in the process per 10 °C change in temperature.

144 2.4 Other measurements

145 Air temperature (T_a , °C), air pressure (P_a , hPa), wind speed (w , m s⁻¹) and water
146 temperatures (T_w , °C), and chlorophyll a concentration ($Chl-a$, µg L⁻¹) were measured every
147 20 minutes during all diel field campaigns. T_a , and P_a were measured using a handheld weather
148 meter (YGY-QXY, China). T_w was measured using a multi-parameter probe (Hydrolab DS5,



149 HACH, US). Water samples were collected at the beginning of each field campaign. These
150 samples were used to measure the concentrations of *Chl-a*, total nitrogen (*TN*) and total
151 phosphorus (*TP*). *Chl-a* was determined by using the national standard method (Wang et al.,
152 2002). *TN* and *TP* were analyzed spectrophotometrically with a continuous flow autoanalyzer
153 (Skalar Analytical, B.V., Breda, Netherlands). Wind speed was measured with a portable aero
154 vane at 2 m height.

155 2.5 Statistical analysis

156 All data were checked for normality using the Kolmogorov-Smirnov test. Pearson's
157 correlations coefficients and linear regressions were used to study the relationships between
158 CH₄ flux and environmental factors. Stepwise linear regressions were performed for relevant
159 combinations of variables. We further estimated seasonal average of variable and defined
160 December, January and February as winter, March to May as spring, June to August as summer,
161 and September to November as autumn.

162 3. Results

163 3.1 Variations in environmental factors

164 Diel and seasonal variations in environmental parameters are summarized in Fig.1. Wind speed
165 was too low to be measured during most campaigns (maximum wind speed was $< 1.5 \text{ m s}^{-1}$)
166 and disregarded from further analysis. Air temperature (T_a) and water temperature (T_w) had
167 significant diel and seasonal changes. The diurnal variation of T_a (ΔT_a) was greater than that
168 of T_w (ΔT_w) (Table 1). The maximum ΔT_a (27.5°C) and ΔT_w (10.1°C) occurred on 28
169 February and the minimum ΔT_a (3.4°C) and ΔT_w (1.3°C) occurred on 20 November. The
170 maximum daily mean air temperature ($\overline{T_a}$) was 29.6°C and was recorded on 17 July, and the



171 minimum value was 5.5°C and was measured on 19 January. The extremes in the daily mean
172 water temperatures ($\overline{T_w}$), 30.5 and 8.6°C, were recorded on 29 August and 19 January (Table
173 1). There were significant seasonal changes of air pressure (Pa) and chlorophyll a ($Chl-a$) (Fig
174 1). The diurnal variation of air pressure (ΔPa) was small. The maximum ΔPa occurred in 29
175 December and the minimum in 27 October. The maximum daily mean air pressure (\overline{Pa}) was
176 recorded on 29 December, and the minimum value was measured on 17 July. Both diurnal and
177 seasonal variations of chlorophyll a ($Chl-a$) ranged widely (Table 1). The maximum diurnal
178 variations of $Chl-a$ occurred in 26 April and the minimum in 29 December. The maximum and
179 the minimum daily mean chlorophyll a ($\overline{Chl-a}$) were recorded on 29 June and 20 November,
180 respectively (27.6 $\mu\text{g L}^{-1}$ to 477.7 $\mu\text{g L}^{-1}$). With TN and TP ranging from 1.36 $\text{mg}\cdot\text{L}^{-1}$ to 5.3
181 $\text{mg}\cdot\text{L}^{-1}$ and 0.04 $\text{mg}\cdot\text{L}^{-1}$ to 0.86 $\text{mg}\cdot\text{L}^{-1}$, respectively, the pond can be classified as eutrophic.
182 Both nutrient concentrations were highest in September (Table 1).

183 We averaged environmental factors in the different seasons and found that T_a , T_w and $Chl-a$
184 were the highest in summer and the lowest in winter, while Pa was the highest in winter and
185 the lowest in summer. There were no significant differences in T_a , T_w , Pa and $Chl-a$ between
186 spring and autumn. TN and TP were highest in autumn and lowest in winter (supplemental
187 Table 1).

188 3.2 CH_4 fluxes

189 *Diffusive CH_4 fluxes*

190 The diffusive flux of CH_4 (D_{CH_4}) from the pond showed obvious but irregular diurnal and
191 seasonal variations (Fig 1). The maximum daily mean diffusive flux ($\overline{D_{\text{CH}_4}}$) was 0.207 ± 0.009
192 $\text{mg CH}_4\cdot\text{m}^{-2}\cdot\text{h}^{-1}$ (mean \pm standard error), observed on 18 May. The minimum $\overline{D_{\text{CH}_4}}$ ($0.011 \pm$



193 0.001 mg CH₄·m⁻²·h⁻¹) was on 20 November. D_{CH_4} was highest in spring (0.146 ± 0.005 mg
194 CH₄·m⁻²·h⁻¹) and lowest in winter (0.103 ± 0.006 mg CH₄·m⁻²·h⁻¹). D_{CH_4} in summer was higher
195 than that in autumn. On average, the daily diffusive CH₄ flux of the pond in 2016 was 2.4 ± 0.5
196 mg CH₄·m⁻²·d⁻¹ (Table 2).

197 The highest diel variability in D_{CH_4} (ΔD_{CH_4}) was observed on 28 February, ranged from
198 0.083 to 0.455 mg CH₄·m⁻²·h⁻¹. The lowest ΔD_{CH_4} was observed on 20 November, ranged from
199 0.005 to 0.022 mg CH₄·m⁻²·h⁻¹. The peak value in 24 h was different during each diel field
200 campaigns. Most of the highest fluxes were observed in the middle of the day or afternoon,
201 when temperatures were higher, such as on 28 February, when D_{CH_4} peaked at 16:00 h. Some
202 of the daily maxima occurred when temperatures began to rise rapidly, such as on 16 July, when
203 D_{CH_4} peaked at 8:30 h. Accordingly, most of the lowest diffusive fluxes occurred at night or
204 early in the morning, when temperatures were lowest or temperatures began to decrease (Fig
205 1).

206 *CH₄ ebullition fluxes*

207 Ebullition mainly occurred from May to September, when CH₄ bubbling was not only more
208 frequent (F_{BCH_4} exceeding 70%) but also more abundant (Fig 1). Variations of CH₄ ebullition
209 were rather random and irregular. Most of the maximum CH₄ ebullition fluxes (B_{CH_4}) during
210 the daily campaign occurred between 0:00 h and 4:00 h, when temperatures were decreasing
211 (such as on 28 February). Some of the maximum B_{CH_4} were observed in the afternoon (between
212 15:00 h and 16:00 h), when temperatures were higher (such as on 17 July), while the maximum
213 B_{CH_4} were observed in the morning (about at 6:00 h), when temperatures were lower during
214 other sampling campaigns (such as on 26 April). The relative frequency of occurrence of CH₄



215 bubbling during the diurnal sampling campaigns (F_{BCH_4}) ranged from 4.2% (observed on 19
216 January and 20 November) to 97.9% (observed on 29 June) (Table 2). Daily total CH_4 ebullition
217 fluxes ranged from 0.3 (on November 20) to 319.9 (on June 29) $mg\ CH_4 \cdot m^{-2} \cdot d^{-1}$. On average,
218 the daily total CH_4 ebullition flux in 2016 was $96.4 \pm 30.5\ mg\ CH_4 \cdot m^{-2} \cdot d^{-1}$.

219 The total daily CH_4 flux ($T_{CH_4} = D_{CH_4} + B_{CH_4}$) ranged from 0.5 (on 20 November) to 322.7
220 (on 29 June) $mg\ CH_4 \cdot m^{-2} \cdot d^{-1}$, and the mean daily T_{CH_4} was $98.7 \pm 30.7\ mg\ CH_4 \cdot m^{-2} \cdot d^{-1}$ (Table
221 2). The contribution of ebullition (B_{CH_4}) to the total flux ranged from 51.8% (on 20 November)
222 to 99.1% (on 29 June). The average daily total CH_4 bubble emissions accounted for 88.6% of
223 the total CH_4 flux (Table 2).

224 3.3 CH_4 fluxes and environmental factors

225 Correlation analysis was conducted for D_{CH_4} and B_{CH_4} obtained from individual chamber
226 deployments, and environmental variables sampled at sub-daily resolution (Table 3). D_{CH_4} was
227 positively correlated ($p < 0.01$) with T_w , T_a and $Chl-a$, while negatively ($p < 0.01$) correlated
228 with Pa and the temperature difference between water and air ($\Delta T = T_w - T_a$). B_{CH_4} was
229 positively correlated with T_w , T_a and $Chl-a$, and negatively correlated with Pa , but not
230 significantly correlated with ΔT ($p = 0.372$). There was a significant positive correlation
231 between D_{CH_4} and B_{CH_4} ($p < 0.01$). We explored potential drivers of D_{CH_4} and B_{CH_4} using
232 stepwise linear regressions (Table 4 and 5). T_a could explain most variations in D_{CH_4} ($r^2 = 0.25$,
233 $p < 0.001$) and the best multiple regression model included T_a , Pa , and B_{CH_4} , which increased
234 the r^2 to 0.28 ($p < 0.001$). T_w could explain most variations in B_{CH_4} ($r^2 = 0.14$, $p < 0.001$) and
235 the best multiple regression model included T_w , $Chl-a$, and ΔT ($r^2 = 0.20$, $p < 0.001$).

236 Correlations between CH_4 fluxes and environmental factors in different seasons were



237 analyzed (Table 3, 4 and 5). The result showed that T_w was the main factor determining CH_4
238 fluxes of the pond in autumn, while $\text{Chl-}a$ was the main factor in summer. Moreover, the main
239 factors determining CH_4 fluxes varied slightly according to CH_4 emission pathway in different
240 season. For diffusion, T_a was the main factor in winter; while T_w and $\text{Chl-}a$ were the main
241 factors in spring. For ebullition, $\text{Chl-}a$ was the main but not strong factor in winter; while the
242 ΔT and T_a were the main factors in spring.

243 We additionally analyzed the relationships between daily total diffusive CH_4 flux (T_{DCH_4}),
244 daily total CH_4 ebullition (T_{BCH_4}), the frequency of daily CH_4 bubbling (F_{BCH_4}) and daily mean
245 values of environmental factors (Table 6). Daily T_{BCH_4} and F_{BCH_4} were positively correlated
246 with each other and both were positively correlated with $\overline{T_w}$, $\overline{T_a}$ and $\overline{\text{Chl-}a}$, while negatively
247 correlated with $\overline{P_a}$. Daily T_{DCH_4} was marginal positively correlated with $\overline{T_w}$, $\overline{T_a}$, T_{BCH_4} and
248 F_{BCH_4} , while negatively correlated with $\overline{P_a}$. Through stepwise regression, we only obtained a
249 model for daily T_{BCH_4} : $T_{\text{BCH}_4} = -110.47 + 10.17 \overline{T_w}$ ($r^2 = 0.49$, $p = 0.011$).

250 The magnitude of the diurnal variation of diffusive CH_4 fluxes (ΔD_{CH_4} is difference between
251 maximum flux and minimum flux), daily total B_{CH_4} , the frequency of daily CH_4 bubbling
252 (F_{BCH_4}) was analyzed with respected to the diel variation of measured parameters (see
253 supplemental Table 2). These analyses showed that ΔD_{CH_4} was positively correlated with ΔT_w
254 and ΔT_a . Through stepwise regression, the best multiple regression model for ΔD_{CH_4} was
255 obtained: $\Delta D_{\text{CH}_4} = 0.01 + 0.036 \Delta T_w$ ($r^2 = 0.63$, $p < 0.001$). F_{BCH_4} was positively correlated
256 with ΔD_{CH_4} , and daily total B_{CH_4} was positively correlated with F_{BCH_4} . Although daily total
257 B_{CH_4} was not significantly correlated with ΔT_w , we found larger ebullition rates for larger Δ
258 T_w for conditions with nearly equal water temperature. For example, the daily mean T_w on 28



259 February (16.1°C) was close to that on 25 March (16.3°C), yet ΔT_w on 28 February was much
260 higher (10.1°C) than that on 25 March (2.8°C). As a result, daily amount of CH₄ ebullition on
261 28 February (T_{BCH_4} , 52.0 mg CH₄·m⁻²·d⁻¹) was obviously higher than that on 25 March (18.3
262 mg CH₄·m⁻²·d⁻¹). This phenomenon was also seen on 29 December and 19 January (Table 1 and
263 2).

264 3.4 Influence of temperature on diffusion and ebullition

265 We bin-averaged gas fluxes according to the temperature difference between the surface
266 water and air ($\Delta T = T_w - T_a$) (Fig 2). The results showed that under $\Delta T < 0$ °C, there was a
267 significant negative linear relationship between D_{CH_4} and ΔT ($R^2 = 0.70$). While ΔT was
268 positive but smaller than 5 °C, D_{CH_4} increased slowly. When ΔT was exceeding 5 °C, D_{CH_4}
269 decreased. Besides, when ΔT was nearly zero ($-1 < \Delta T < 1$ °C), the averaged diffusive CH₄
270 fluxes (0.091 ± 0.011 mg CH₄·m⁻²·h⁻¹) was not significantly different from the mean diffusive
271 CH₄ flux for the entire year (0.098 ± 0.019 mg CH₄·m⁻²·h⁻¹). We also compared the averaged
272 diffusive CH₄ fluxes under $-1 < \Delta T < 1$ °C with daily mean diffusive CH₄ flux each month
273 (See supplemental Table 3), and found that there were no significant differences between them
274 except for 29 August.

275 CH₄ ebullition (B_{CH_4}) and the frequency of CH₄ bubbling (F_{BCH_4}) under different ΔT
276 showed that when ΔT was near zero ($-1 < \Delta T < 1$ °C), F_{BCH_4} was about 30%, and ebullition
277 ranged between 117 ~ 136 mg CH₄·m⁻²·d⁻¹, which was close to the average CH₄ ebullition flux
278 (96.4 ± 30.5 mg CH₄·m⁻²·d⁻¹). When $\Delta T > 1$ °C and $\Delta T < -1$ °C, F_{BCH_4} started to increase.
279 Meanwhile the ebullition flux increased substantially when $1 < \Delta T < 5$ °C and $-3 < \Delta T < -1$
280 °C; yet when $\Delta T > 5$ °C and $\Delta T < -3$ °C, the bubbling flux decreased sharply (Fig. 3).



281 3.5 Temperature dependency of CH₄ fluxes

282 Temperature was the strongest predictor for seasonal variations of D_{CH_4} and B_{CH_4} . We
283 calculated the temperature dependence of CH₄ fluxes in terms of Q_{10} (Fig 4). The results
284 showed that the Q_{10} of daily total D_{CH_4} of $\overline{T_w}$ and $\overline{T_a}$ were 2.05 and 1.87, respectively. While
285 the Q_{10} of daily total B_{CH_4} of $\overline{T_w}$ and $\overline{T_a}$ were 5.52 and 4.38, respectively.

286 We further explored Q_{10} of ebullition and diffusive emissions for a range of TP
287 concentrations (Table 7). Both ebullition and diffusion responded slightly stronger to T_w than
288 to T_a regardless of TP concentrations. For diffusion, Q_{10} increased with TP concentration when
289 the averaged TP was below $0.4 \text{ mg}\cdot\text{L}^{-1}$. For example, when the averaged TP was $0.05 \text{ mg}\cdot\text{L}^{-1}$,
290 the Q_{10} of the diffusive CH₄ flux for T_w and T_a were 1.29 and 1.27, respectively. When the
291 averaged TP was $0.4 \text{ mg}\cdot\text{L}^{-1}$, the Q_{10} of the diffusive CH₄ flux to T_w and T_a increased to 7.52
292 and 5.23, respectively. However, when averaged TP was higher than $0.8 \text{ mg}\cdot\text{L}^{-1}$, its Q_{10} tended
293 to decline. For ebullition, although there was no exponential relationship when TP was $0.2 \sim$
294 $0.4 \text{ mg}\cdot\text{L}^{-1}$, Q_{10} also tended to increase with TP concentration. For example, when averaged TP
295 was $0.05 \text{ mg}\cdot\text{L}^{-1}$, Q_{10} of CH₄ ebullition flux to T_w and T_a were 1.32 and 1.15, respectively.
296 When averaged TP was exceeding $0.8 \text{ mg}\cdot\text{L}^{-1}$, Q_{10} increased to 3.29 and 2.06, respectively.

297 4. Discussion

298 4.1 Contribution of diffusion and ebullition to total CH₄ emissions

299 The diffusive CH₄ fluxes from the studied pond were on average $2.36 \pm 0.07 \text{ mg CH}_4\cdot\text{m}^{-2}\cdot\text{d}$
300 ¹, which is close to the mean diffusive CH₄ fluxes of ponds and small lakes with sizes between
301 0.1 and 1 km^2 ($2.56 \text{ mg CH}_4 \text{ m}^{-2}\cdot\text{d}^{-1}$, Holgerson and Raymond, 2016). However, the diffusive
302 CH₄ fluxes were lower than what has been reported. The diffusive fluxes from a shallow



303 eutrophic lake in southern Brazil, estimated from summer and winter, were 9.35 and 2.17 mg
304 $\text{CH}_4 \text{ m}^{-2} \cdot \text{d}^{-1}$, respectively (Palma-Silva et al., 2013). The mean diffusive flux from a tropical
305 pond in India was 49.6 mg $\text{CH}_4 \text{ m}^{-2} \cdot \text{d}^{-1}$ (the high diffusive flux from one pond was 324.8 mg
306 $\text{CH}_4 \text{ m}^{-2} \cdot \text{d}^{-1}$) (Panneer Selvam et al., 2014). DelSontro et al. (2016) found an average diffusive
307 CH_4 flux of 57.6 mg $\text{CH}_4 \text{ m}^{-2} \cdot \text{d}^{-1}$ (from May to November) from ten shallow and vegetated
308 beaver ponds in Canada, which was more than one order of magnitude higher than the diffusive
309 fluxes observed in the present study.

310 CH_4 ebullition fluxes both in summer and winter in the study (See supplemental Table 1)
311 ranged within the bubble CH_4 emissions reported by PalmaSilva et al. (2013) from a shallow
312 eutrophic lake in southern Brazil. The average CH_4 ebullition flux in our study was 96.4 ± 30.5
313 mg $\text{CH}_4 \cdot \text{m}^{-2} \cdot \text{d}^{-1}$, comparable to the mean ebullition flux from the tropical region in India (112
314 mg $\text{m}^{-2} \cdot \text{d}^{-1}$) (Panneer Selvam et al., 2014), while obviously higher than the fluxes reported from
315 lakes in northern Sweden (22.0 mg $\text{CH}_4 \cdot \text{m}^{-2} \cdot \text{d}^{-1}$) (Wik et al., 2013), shallow beaver ponds in
316 Canada (73.6 mg $\text{CH}_4 \cdot \text{m}^{-2} \cdot \text{d}^{-1}$) (DelSontro et al., 2016), and eight small thaw ponds in northern
317 Sweden (20.0 mg $\text{CH}_4 \cdot \text{m}^{-2} \cdot \text{d}^{-1}$) (Burke et al., 2019), all of which are located at high latitudes.

318 The mean total CH_4 flux of the pond (T_{CH_4}) during the whole field investigations was 98.7
319 $[0.5 - 322.7] \pm 30.7 \text{ mg} \cdot \text{CH}_4 \cdot \text{m}^{-2} \cdot \text{d}^{-1}$ (mean [range] \pm SD, Table 2), which was lower than the
320 ponds (286.4 [3.2 - 833.6] mg $\cdot \text{CH}_4 \cdot \text{m}^{-2} \cdot \text{d}^{-1}$), and higher than the lakes (64 [0.32 - 284.8]
321 mg $\cdot \text{CH}_4 \cdot \text{m}^{-2} \cdot \text{d}^{-1}$) from the tropical region in India (Panneer Selvam et al., 2014) and from a
322 small shallow pond in Sweden (128 [52.8 - 241.6] mg $\cdot \text{CH}_4 \cdot \text{m}^{-2} \cdot \text{d}^{-1}$) (Natchimuthu et al., 2014).
323 A growing body of research has found that ebullition contributed largely to the total CH_4
324 emissions, such as on average 91 % of the total CH_4 emissions from a small pond in Sweden



325 (its average depth was 1.2 m) (Natchimuthu et al., 2014), 56% from the beaver ponds in Canada
326 (DelSontro et al., 2016), 75% from forty-five aquatic systems in the tropical region of India
327 (Panneer Selvam et al., 2014), and 40–60 % in lakes (Bastviken et al., 2004). In our study,
328 the average contributions of CH₄ ebullition to the total CH₄ flux was at the higher range of
329 observations (88.6%), indicating that ebullition played a major role in CH₄ emissions from the
330 shallow pond studied here. The result confirms that ebullition is an important pathway for CH₄
331 transport to the atmosphere in shallow aquatic systems, such as ponds (Casper et al., 2000;
332 DelSontro et al., 2016). The larger importance of ebullition in shallow water can be related to
333 the low hydrostatic pressure in the sediment (Bastviken et al., 2004), which reduces the
334 dissolved gas concentration that is required for bubble formation.

335 Eutrophication could be a contributing factor in the relatively high contribution of ebullition
336 to overall CH₄ flux in our study. The pond studied here was highly eutrophic, with *TP*, *TN* and
337 *Chl-a* exceeding those observed for the beaver ponds in Canada (DelSontro et al., 2016).
338 Eutrophic systems tend to accumulate more organic carbon (Anderson et al., 2014). When
339 substrate is not limiting, there is a greater potential for CH₄ ebullition, thus leading to higher
340 total CH₄ emissions as bubbles directly transport CH₄ to the atmosphere with limited exposure
341 to oxidation (DelSontro et al., 2010).

342 4.2 Influence of temperature on CH₄ flux

343 Many studies, including field measurements, indicated that temperature affects CH₄
344 emissions (Duc et al., 2010; Xing et al., 2005; Natchimuthu et al., 2014; Wik et al., 2014; Aben
345 et al., 2017). In our case, both diffusive and ebullition CH₄ fluxes were positively correlated
346 with *T_w* and *T_a*. For example, variations in *T_w* explained as much as 71 % of the variation in



347 diffusion and 33 % of the variation in ebullition in autumn and variations in T_a explained 54 %
348 of the variation in diffusion in winter. Besides, diurnal variation of T_w (ΔT_w) explained 63 %
349 of the variation of the diurnal pattern of diffusive CH_4 emissions (ΔD_{CH_4}). Altogether, our
350 findings confirm that temperature is among the strongest predictors for CH_4 emissions.
351 Methanogenesis is highly temperature dependent (Zimov et al., 1997; Van Hulzen et al., 1999),
352 and higher temperature results in higher CH_4 production rates. In our study, the correlation
353 between T_w and diffusive CH_4 flux was almost as strong that with T_a . Yet, ebullition was more
354 strongly correlated with T_w than T_a (Table 3 and Table 6), variations in daily $\overline{T_w}$ explained
355 49 % of the variation in daily total CH_4 ebullition ($p = 0.011$). Wik et al. (2014) determined
356 sediment temperature to be a significant driver of ebullitive CH_4 flux from shallow lakes.
357 Although the temperature of sediment was not measured in our study, it was mainly controlled
358 by water temperature. For shallow ponds, CH_4 is mainly formed in anoxic sediments, and
359 sediment temperature is likely to increase with air and water temperature. CH_4 emissions may
360 increase with increasing temperature due to the direct temperature effect on methanogenesis in
361 shallow sediments (Bastviken et al., 2008). In addition, ebullition dominated the CH_4 emission
362 in our pond, which might be another reason that CH_4 flux depends on the temperature. Because
363 ebullition largely escapes methane oxidation in the system, it is more directly related to
364 methane production rates in sediments than diffusive emissions (Natchimuthu et al., 2014;
365 Wilkinson et al., 2015). Thus, ebullition responds more directly to T_w because of the
366 stimulatory effects of high temperature on methanogenesis without the confounding effect of
367 methane oxidation.

368 Convective mixing during nighttime cooling of the water column has been found to coincide



369 with pulses of CH₄ emissions in wetlands (Poindexter, 2016). When the difference between
370 water and air temperature was positive, the diffusive gas fluxed can be expected to be enhanced
371 by high gas exchange velocities (MacIntyre et al., 2001). In our study, when $0 < \Delta T < 5$ °C,
372 the diffusive CH₄ flux increased slowly, but CH₄ ebullition increased substantially, indicating
373 that the CH₄ flux might be strongly enhanced due to thermal convection. However, when ΔT
374 was exceeding 5 °C, both diffusion and ebullition tended to decrease. That time was mainly
375 concentrated in the early morning, the temperature was usually the lowest, and lower CH₄ flux
376 was mainly limited by low temperature. When $\Delta T < -3$ °C, the bubbling flux decreased sharply,
377 while diffusive CH₄ flux increased linearly, indicating that diffusion was an important pathway
378 for CH₄ transport to the atmosphere when the weather was sunny, and air temperature increased
379 more quickly than water temperature. Furthermore, when air temperature was close to water
380 temperature, diffusive fluxes and ebullition were close to their long-term mean values.

381 4.3 Effects of eutrophication on temperature dependence of CH₄ fluxes

382 We calculated the temperature dependence of CH₄ fluxes in terms of the temperature
383 coefficient Q_{10} , which was defined by DelSontro et al. (2016) as an “ecosystem-level” Q_{10} ,
384 representing the combining effects of multiple biotic and abiotic factors. Q_{10} values in beaver
385 ponds varied slightly according to CH₄ emission pathway and bubbling appeared to be more
386 sensitive to temperature than the diffusive pathway (DelSontro et al., 2016). In our study, the
387 Q_{10} of CH₄ diffusion in respect to $\overline{T_w}$ and $\overline{T_a}$ were 2.05 and 1.87, respectively; while the Q_{10}
388 of CH₄ ebullition of $\overline{T_w}$ and $\overline{T_a}$ were 5.52 and 4.38, respectively. Our values were
389 comparable to those estimated for subtropical and temperate eutrophic city ponds (Q_{10} ranged
390 from 1.63 ~ 6.73) (Aben et al., 2017). In contrast to the beaver ponds in Canada, whose average



391 Q_{10} values for ebullition and diffusion fluxes to sediment temperature were 13 and 10,
392 respectively (DelSontro et al., 2016), our Q_{10} values were lower. Our study also showed that
393 there was a higher temperature sensitivity of bubbling from the ponds, compared to diffusive
394 fluxes. The reason could be due to its very shallow nature and shallow sediment layer, which
395 could cause frequent ebullition and thus promote a more erratic ebullition versus temperature
396 pattern (Wik et al., 2018).

397 The strong temperature dependence of CH_4 fluxes in our study might be related to its higher
398 productivity. High nutrient concentration promotes the productivity and algal growth (West et
399 al., 2012). The study from the beaver ponds in Canada showed that the temperature dependence
400 of CH_4 fluxes increased with TP , and the temperature dependence of ebullition was
401 disproportionately enhanced by ecosystem productivity relative to diffusion (DelSontro et al.,
402 2016). The authors pointed out that as system productivity and the supply of organic matter
403 increased, the CH_4 production was increasingly regulated by temperature (DelSontro et al.,
404 2016). A mesocosm-based study in shallow aquatic systems revealed synergistic effect from
405 combination of nutrient enrichment and experimental warming, causing an increasing mean
406 annual ebullition rate; while the diffusive flux remained unaffected by nutrient enrichment but
407 had a largely positive response to temperature treatment (Davidson, 2018). In our case, Q_{10} of
408 both ebullitive and diffusive fluxes increased with system TP within a certain TP range.
409 However, the temperature dependence of diffusive fluxes was more sensitive to ecosystem
410 productivity when compared to ebullition. A likely reason for this may be the low frequency of
411 bubbles, which needs more work to be verified.

412 **5. Conclusions**



413 The subtropical, shallow, small and eutrophic pond emitted on average $98.7 \pm 30.7 \text{ mg} \cdot \text{m}^{-2} \cdot \text{d}^{-1}$ of CH_4 . Ebullition was quantitatively most important, accounting for 51.8% to 99.1% of
414
415 the total CH_4 emission. A positive correlation between temperature and CH_4 fluxes shows that
416 there are likely positive feedbacks of aquatic CH_4 fluxes to global warming. The temperature
417 dependence of the CH_4 fluxes increased with increasing nutrient concentration. By combing
418 these facts, we conclude that the increasing cultural eutrophication and global warming
419 promote increasing atmospheric CH_4 emissions from these vastly abundant aquatic
420 ecosystems.

421 6. Data availability

422 The data published in this contribution can be accessed by email request to the corresponding
423 author.

424 7. Author contribution

425 In this work, W.L.Z analyzed the data and wrote the article, S.B.X designed the experiment,
426 H.X, J.L and D.L performed the experiment, and A.L revised the article.

427 8. Competing interests

428 The authors declare that they have no conflict of interest.

429 Acknowledgements

430 This work was financially supported by the National Science Foundation of China (No.
431 41273110), Natural Science Foundation of Hubei Province, China (2014CFB672), and Hubei
432 Provincial Department of Education Scientific research projects (Q20151209). The Hubei
433 province Chutian Scholar program (granted to AL) provided additionally financial support for
434 this study. We thank Li Long and Junwei Zhang for their help with fieldwork.



435 **References**

- 436 Aben, R. C. H., Barros, N., Donk, E. V., Frenken, T., Hilt, S., Kazanjian, G., Lamers, L. P. M.,
437 Peeters, E. T. H. M., Roelofs, J. G. M., Domis, L. N. d. S., Stephan, S., Velthuis, M.,
438 Van de Waal, D. B., Wik, M., Thornton B. F., Wilkinson, J., DelSontro, T., and Kosten,
439 S.: Cross continental increase in methane ebullition under climate change., Nature
440 communications, 8, [https://doi.org/ 10.1038/s41467-017-01535-y](https://doi.org/10.1038/s41467-017-01535-y), 2017.
- 441 Anderson, N. J., Bennion, H., and Lotter, A. F.: Lake eutrophication and its implications for
442 organic carbon sequestration in Europe, Glob Chang Biol, 20, 2741-2751,
443 [https://doi.org/ 10.1111/gcb.12584](https://doi.org/10.1111/gcb.12584), 2014.
- 444 Bastviken, D., Cole, J., Pace, M., and Tranvik, L.: Methane emissions from lakes: Dependence
445 of lake characteristics, two regional assessments, and a global estimate, Global
446 Biogeochemical Cycles, 18, [https://doi.org/ 10.1029/2004GB002238](https://doi.org/10.1029/2004GB002238), 2004.
- 447 Bastviken, D., Cole, J. J., Pace, M. L., and Van de Bogert, M. C.: Fates of methane from
448 different lake habitats: Connecting whole-lake budgets and CH₄ emissions, Journal of
449 Geophysical Research, 113, [https://doi.org/ 10.1029/2007JG000608](https://doi.org/10.1029/2007JG000608), 2008.
- 450 Bastviken, D., Tranvik, L. J., Downing, J. A., Crill, P. M., and Enrich-Prast, A.: Freshwater
451 Methane Emissions Offset the Continental Carbon Sink, Science, 331, 50-50,
452 [https://doi.org/ 10.1126/science.1196808](https://doi.org/10.1126/science.1196808), 2011.
- 453 Burger, M., Berger, S., Spangenberg, I., and Blodau, C.: Summer fluxes of methane and carbon
454 dioxide from a pond and floating mat in a continental Canadian peatland,
455 Biogeosciences, 13, 3777–3791. [https://doi.org/ 10.5194/bg-13-3777-2016](https://doi.org/10.5194/bg-13-3777-2016), 2016.
- 456 Burke, S. A., Wik, M., Lang, A., Contosta, A. R., Palace, M., Crill, P. M., and Varner, R. K.:



- 457 Long - Term Measurements of Methane Ebullition From Thaw Ponds, Journal of
458 Geophysical Research: Biogeosciences, 124, 14, [https://doi.org/](https://doi.org/10.1029/2018jg004786)
459 10.1029/2018jg004786, 2019.
- 460 Casper, P., Maberly, S. C., Hall, G. H., and Finlay, P. J.: Fluxes of methane and carbon dioxide
461 from a small productive lake to the atmosphere, Biogeochemistry, 49, 1-19,
462 [https://doi.org/ 10.2307/1469408](https://doi.org/10.2307/1469408), 2000.
- 463 Davidson, T. A., Audet, J., Svenning, J.-C., Lauridsen, T. L., Søndergaard, M., Landkildehus,
464 F., Larsen, S. E., and Jeppesen, E.: Eutrophication effects on greenhouse gas fluxes
465 from shallow-lake mesocosms override those of climate warming, Global Change
466 Biology, 21, <https://doi.org/10.1111/gcb.13062>, 2015.
- 467 Davidson, T. A., Audet J., Jeppesen E., Landkildehus F., Lauridsen T. L., Søndergaard M. and
468 Syväranta J.: Synergy between nutrients and warming enhances methane ebullition
469 from experimental lakes, Nature Climate Change, 8, 5, [https://doi.org/10.1038/s41558-](https://doi.org/10.1038/s41558-017-0063-z)
470 017-0063-z, 2018.
- 471 DelSontro, T., McGinnis, D. F., Sobek, S., Ostrovsky, I., and Wehrli, B.: Extreme Methane
472 Emissions from a Swiss Hydropower Reservoir: Contribution from Bubbling
473 Sediments, Environmental Science & Technology, 44, 2419-2425,
474 <https://doi.org/10.1021/es9031369>, 2010.
- 475 DelSontro, T., Boutet, L., St-Pierre, A., del Giorgio, P. A., and Prairie, Y. T.: Methane ebullition
476 and diffusion from northern ponds and lakes regulated by the interaction between
477 temperature and system productivity, Limnology and Oceanography, 61, S62-S77,
478 [https://doi.org/ 10.1002/lno.10335](https://doi.org/10.1002/lno.10335), 2016.



- 479 Downing, J. A., Prairie, Y. T., Cole, J. J., Duarte, C. M., Tranvik, L. J., Striegl, R. G., McDowell,
480 W. H., Kortelainen, P., Caraco, N. F., Melack, J. M., and Middelburg, J. J.: The global
481 abundance and size distribution of lakes, ponds, and impoundments, *Limnology and*
482 *Oceanography Methods*, 51, 2388-2397, <https://doi.org/10.4319/lo.2006.51.5.2388>,
483 2006.
- 484 Downing, J. A., Cole, J. J., Middelburg, J. J., Striegl, R. G., Duarte, C. M., Kortelainen, P.,
485 Prairie, Y. T., and Laube, K. A.: Sediment organic carbon burial in agriculturally
486 eutrophic impoundments over the last century, *Global Biogeochemical Cycles*, 22,
487 <https://doi.org/10.1029/2006gb002854>, 2008.
- 488 Duc, N., Crill, P., and Bastviken, D.: Implications of temperature and sediment characteristics
489 on methane formation and oxidation in lake sediments, *Biogeochemistry*, 100, 185-196,
490 <https://doi.org/10.1007/s10533-010-9415-8>, 2010.
- 491 Hamilton, J. D., and Kelly, C. A.: Flux to the atmosphere of CH₄ and from wetland ponds on
492 the Hudson Bay lowlands (HBLs), *Journal of geophysical research*, 99, 16,
493 https://doi.org/10.1029_93JD03020, 1994.
- 494 Hanson, P. C., Carpenter, S. R., A., C. J., and Winslow, L. A.: Small lakes dominate a random
495 sample of regional lake characteristics, *Freshwater Biology*, 52, 9,
496 <https://doi.org/10.1111/j.1365-2427.2007.01730.x>, 2007.
- 497 Holgerson, M. A.: Drivers of carbon dioxide and methane supersaturation in small, temporary
498 ponds, *Biogeochemistry*, 124, 305-318, <https://doi.org/10.1007/s10533-015-0099-y>,
499 2015.
- 500 Holgerson, M. A., and Raymond, P. A.: Large contribution to inland water CO₂ and CH₄



501 emissions from very small ponds, *Nature Geoscience*, 9, 222-226,
502 <https://doi.org/10.1038/ngeo2654>, 2016.

503 Houghton, J. T., Ding, Y., Griggs, D. J., Noguera, M., van der Linden, P. J., Dai, X., Maskell, K.,
504 and Johnson, C. A.: IPCC 2001, *Climate Change 2001: The Scientific Basis*, University
505 Press Cambridge, 2001.

506 IPCC: *Climate Change 2014: Synthesis Report. Contribution of Working Groups I, II and III*
507 *to the Fifth Assessment Report of the Intergovernmental Panel on Climate Change*
508 [Core Writing Team, R.K. Pachauri and L.A. Meyer (eds.)]. IPCC, 151, 2014.

509 Kankaala, P., Huotari, J., TOLONEN, T., and Ojala, A.: Lake-size dependent physical forcing
510 drives carbon dioxide and methane effluxes from lakes in a boreal landscape,
511 *Limnology and Oceanography*, 58, 1915–1930, [https://doi.org/](https://doi.org/10.4319/lo.2013.58.6.1915)
512 [10.4319/lo.2013.58.6.1915](https://doi.org/10.4319/lo.2013.58.6.1915), 2013.

513 Kirschke, S., Bousquet, P., Ciais, P., Saunoy, M., Canadell, J. G., Dlugokencky, E. J.,
514 Bergamaschi, P., Bergmann, D., Blake, D. R., Bruhwiler, L., Cameron-Smith, P.,
515 Castaldi, S., Chevallier, F., Feng, L., Fraser, A., Heimann, M., Hodson, E. L.,
516 Houweling, S., Josse, B., Fraser, P. J., Krummel, P. B., Lamarque, J.-F., Langenfelds,
517 R. L., Le Quéré, C., Naik, V., O’Doherty, S., Palmer, P. I., Pison, I., Plummer, D.,
518 Poulter, B., Prinn, R. G., Rigby, M., Ringeval, B., Santini, M., Schmidt, M., Shindell,
519 D. T., Simpson, I. J., Spahni, R., Steele, L. P., Strode, S. A., Sudo, K., Szopa, S., van
520 der Werf, G. R., Voulgarakis, A., van Weele, M., Weiss, R. F., Williams, J. E., and Zeng,
521 G.: Three decades of global methane sources and sinks, *Nature geoscience*, 6, 813–823,
522 [https://doi.org/ 10.1038/NGEO1955](https://doi.org/10.1038/NGEO1955), 2013.



- 523 Lambert, M., and Fréchet, J.: Analytical techniques for measuring fluxes of CO₂ and CH₄
524 from hydroelectric reservoirs and natural water bodies, in: Greenhouse Gas
525 Emissions—Fluxes and Processes: Hydroelectric Reservoirs and Natural Environments,
526 edited by: Tremblay, A., Varfalvy, L., Roehm, C., and Garneau, M., Springer, Berlin,
527 37-60, 2005.
- 528 Loulergue, L., Schilt, A., Spahni, R., Masson-Delmotte, V. r., Blunier, T., Lemieux, B. n. d.,
529 Barnola, J.-M., Raynaud, D., Stocker, T. F., and Chappellaz, J. r. m.: Orbital and
530 millennial-scale features of atmospheric CH₄ over the past 800,000 years, Nature letters,
531 453, 383–386, <https://doi.org/10.1038/nature06950>, 2008.
- 532 Lundin, E. J. , Giesler, R. , Persson, A. , Thompson, M. S. , and Karlsson, J. : Integrating carbon
533 emissions from lakes and streams in a subarctic catchment. Journal of Geophysical
534 Research: Biogeocences, 118, 3, <https://doi.org/10.1002/jgrg.20092>, 2013.
- 535 MacIntyre, S., Eugster, W., and Kling, G. W.: The critical importance of buoyancy flux for gas
536 flux across the air-water interface, AGU Geophysical Monograph, 127, 5, 135–139,
537 <https://doi.org/10.1029/GM127p0135>, 2001.
- 538 Natchimuthu, S., Panneer Selvam, B., and Bastviken, D.: Influence of weather variables on
539 methane and carbon dioxide flux from a shallow pond, Biogeochemistry, 119, 403–413,
540 <https://doi.org/10.1007/s10533-014-9976-z>, 2014.
- 541 Palma-Silva, C., Marinho, C. C., Albertoni, E. F., Giacomini, I. B., Figueiredo Barros, M. P.,
542 Furlanetto, L. M., Trindade, C. R. T., and Esteves, F. d. A.: Methane emissions in two
543 small shallow neotropical lakes: The role of temperature and trophic level, Atmospheric
544 Environment, 81, 373-379, <http://dx.doi.org/10.1016/j.atmosenv.2013.09.029>, 2013.



- 545 Panneer Selvam, B., Natchimuthu, S., Arunachalam, L., and Bastviken, D.: Methane and
546 carbon dioxide emissions from inland waters in India – implications for large scale
547 greenhouse gas balances, *Global Change Biology*, 20, 3397-3407,
548 <https://doi.org/10.1111/gcb.12575>, 2014.
- 549 Peixoto, R. B., Machado-Silva, F., Marotta, H., Enrich-Prast, A., and Bastviken, D.: Spatial
550 versus day-to-day within lake variability in tropical floodplain lake CH₄ emissions—
551 developing optimized approaches to representative flux measurements, *PLoS One*, 10,
552 <https://doi.org/10.1371/journal.pone.0123319>., 2015.
- 553 Poindexter, C. M., D. D. Baldocchi, J. H. Matthes, S. H. Knox, and E. A. Variano.: The
554 contribution of an overlooked transport process to a wetland's methane emissions,
555 *Geophys. Res. Lett.*, 43, 9, <https://doi.org/10.1002/2016GL068782>, 2016.
- 556 Rasilo, T., Prairie, Y. T., and Del Giorgio, P. A.: Large-scale patterns in summer diffusive CH₄
557 fluxes across boreal lakes, and contribution to diffusive C emissions, *Global Change*
558 *Biology*, 21, 16, <https://doi.org/10.1111/gcb.12741>, 2015.
- 559 Van Hulzen, J. B., Segers, R., van Bodegom, P. M., and Leffelaar, P. A.: Temperature effects
560 on soil methane production: an explanation for observed variability, *Soil Biology &*
561 *biochemistry*, 31, 1919–1929. [https://doi.org/10.1016/s0038-0717\(99\)00109-1](https://doi.org/10.1016/s0038-0717(99)00109-1), 1999.
- 562 Wang, X. F., Wei, F. S., and Qi, W. Q.: *Monitoring and Analysis Methods of Water and*
563 *Wastewater (the fourth edition)*. China Environmental Science Press, Beijing (in
564 Chinese), 2002.
- 565 West, W. E., Coloso, J. J., and Jones, S. E.: Effects of algal and terrestrial carbon on methane
566 production rates and methanogen community structure in a temperate lake sediment,



567 Freshwater Biology, 57, 949-955, <https://doi.org/10.1111/j.1365-2427.2012.02755.x>,
568 2012.

569 West, W. E., Creamer, K. P., and Jones, S. E.: Productivity and depth regulate lake contributions
570 to atmospheric methane, *Limnology and Oceanography*, 61, S51-S61,
571 <https://doi.org/10.1002/lno.10247>, 2016.

572 Wik, M., Crill, P. M., Varner, R. K., and Bastviken, D.: Multiyear measurements of ebullitive
573 methane flux from three subarctic lakes, *Journal of Geophysical Research:*
574 *Biogeosciences*, 118, 1307-1321, <https://doi.org/10.1002/jgrg.20103>, 2013.

575 Wik, M., Thornton, B. F., Bastviken, D., MacIntyre, S., Varner, R. K., and Crill, P. M.: Energy
576 input is primary controller of methane bubbling in subarctic lakes, *Geophysical*
577 *Research Letters*, 41, 555-560, <https://doi.org/10.1002/2013gl058510>, 2014.

578 Wik, M., Thornton, B. F., Bastviken, D., Uhlbäck, J., and Crill, P. M.: Biased sampling of
579 methane release from northern lakes: A problem for extrapolation, *Geophysical*
580 *Research Letters*, 43, 7, <https://doi.org/10.1002/2015GL066501>, 2016a.

581 Wik, M., Varner, R. K., Anthony, K. W., MacIntyre, S., and Bastviken, D.: Climate-sensitive
582 northern lakes and ponds are critical components of methane release, *Nature geoscience*
583 9, 7, <https://doi.org/10.1038/NGEO2578>, 2016b.

584 Wik, M., Johnson, J. E., Crill, P. M., DeStasio, J. P., Erickson, L., Halloran, M. J., Fahnestock,
585 M. F., Crawford, M. K., Phillips, S. C., and Varner, R. K.: Sediment Characteristics and
586 Methane Ebullition in Three Subarctic Lakes, *Journal of Geophysical Research:*
587 *Biogeosciences*, 123, 2399-2411, <https://doi.org/10.1029/2017jg004298>, 2018.

588 Wilkinson, J., Maeck, A., Alshboul, Z., and Lorke, A.: Continuous Seasonal River Ebullition



589 Measurements Linked to Sediment Methane Formation, *Environmental Science &*
590 *Technology*, 49, 13121-13129, <https://doi.org/10.1021/acs.est.5b01525>, 2015.

591 Xiao, S., Yang, H., Liu, D., Zhang, C., Lei, D., Wang, Y., Peng, F., Li, Y., Wang, C., Li, X., Wu,
592 G., and Liu, L.: Gas transfer velocities of methane and carbon dioxide in a subtropical
593 shallow pond, *Tellus B: Chemical and Physical Meteorology*, 66, 23795,
594 <https://doi.org/10.3402/tellusb.v66.23795>, 2014.

595 Xing, Y., Xie, P., Yang, H., Ni, L., Wang, Y., and Rong, K.: Methane and carbon dioxide fluxes
596 from a shallow hypereutrophic subtropical Lake in China, *Atmospheric Environment*,
597 39, 5532-5540, <https://doi.org/10.1016/j.atmosenv.2005.06.010>, 2005.

598 Zimov, S. A., Voropaev, Y. V., Semiletov, I. P., Davidov, S. P., Prosiannikov, S. F., Chapin, I. F.
599 S., Chapin, M. C., Trumbore, S., and Tyler, S.: North Siberian Lakes: a methane source
600 fueled by Pleistocene carbon, *Sciences*, 227, 800-802,
601 <https://www.jstor.org/stable/2893123>, 1997.
602



603 Table 1 Daily averaged and diurnal variation of physical and chemical characteristics for each
 604 sampling date. Daily mean air temperature ($\overline{T_a}$), daily mean water temperatures ($\overline{T_w}$), daily
 605 mean air pressure ($\overline{P_a}$), daily mean chlorophyll a ($\overline{Chl-a}$), diurnal variation of T_a (ΔT_a),
 606 diurnal variation of T_w (ΔT_w), diurnal variation of air pressure (ΔP_a), diurnal variation of
 607 chlorophyll a ($\Delta Chl-a$), daily mean total nitrogen (\overline{TN}) and daily mean total phosphorus (\overline{TP}).

608 Note: TN and TP were invalid on 29 December.

609

Date	$\overline{T_a}$ (°C)	$\overline{T_w}$ (°C)	$\overline{P_a}$ (hPa)	$\overline{Chl-a}$ ($\mu\text{g L}^{-1}$)	ΔT_a (°C)	ΔT_w (°C)	ΔP_a (hPa)	$\Delta Chl-a$ ($\mu\text{g L}^{-1}$)	\overline{TP} (mg L^{-1})	\overline{TN} (mg L^{-1})
Jan 19	5.5	8.6	1019	181.3	4.8	1.3	5.1	143	0.04	2.13
Feb 28	15.8	16.1	1013	96.9	27.5	10.1	6.9	81	0.04	2.13
Mar 25	12.8	16.3	1020	180.6	15.0	2.8	4.3	134	0.13	2.98
Apr 26	19.3	21.2	1003	311.6	6.1	2.2	3.0	1091	0.22	2.49
May 18	22.7	24.8	1003	256.7	12.9	3.8	3.5	564	0.33	3.34
Jun 29	24.9	26.5	998	477.7	10.1	3.8	3.1	663	0.10	2.81
Jul 17	29.6	29.4	995	211.2	9.5	5.7	4.0	366	0.07	1.36
Aug 29	25.8	30.5	1003	181.1	15.0	7.4	3.9	341	0.34	3.39
Sep 24	26.3	26.2	1003	420.6	9.7	3.3	3.5	567	0.86	5.30
Oct 27	15.6	17.8	1010	261.5	4.3	1.6	2.9	261	0.86	5.30
Nov 20	16.2	16.9	1009	27.6	3.4	1.3	6.4	76	0.56	4.09
Dec 29	5.7	9.5	1024	53.9	14.6	4.2	9.4	61	----	----

610

611



612 Table 2 Daily total diffusive CH₄ flux (T_{DCH_4}), diel variability in D_{CH_4} (ΔD_{CH_4}),
 613 frequency of daily CH₄ bubbling (F_{BCH_4}), daily total CH₄ ebullition flux (T_{BCH_4}),
 614 and daily total CH₄ flux (T_{CH_4}) for all sampling campaigns. Bold letters indicated
 615 larger ebullition rates for larger ΔT_w for conditions with nearly equal water
 616 temperature.
 617

Date	ΔD_{CH_4} (mg·m ⁻² ·d ⁻¹)	T_{DCH_4} (mg·m ⁻² ·d ⁻¹)	F_{BCH_4} (%)	T_{BCH_4} (mg·m ⁻² ·d ⁻¹)	T_{CH_4} (mg·m ⁻² ·d ⁻¹)	T_{BCH_4}/T_{CH_4} (%)
Dec 29	0.03	0.5	39.6	43.6	44.2	98.8
Jan 19	0.07	1.8	4.2	3.8	5.6	67.8
Feb 28	0.37	4.1	45.8	52.0	56.1	92.6
Mar 25	0.09	1.5	12.5	18.3	19.8	92.4
Apr 26	0.12	2.8	10.4	6.8	9.6	71.1
May 18	0.33	5.0	89.6	235.2	240.2	97.9
Jun 29	0.17	2.7	97.9	319.9	322.7	99.1
Jul 17	0.18	3.2	72.9	134.5	137.8	97.6
Aug 29	0.27	4.2	70.8	149.4	156.7	97.2
Sep 24	0.15	1.7	93.8	174.5	176.3	99.0
Oct 27	0.02	0.4	27.1	17.9	18.3	97.8
Nov 20	0.02	0.3	4.2	0.3	0.5	51.8
All	0.2	2.4±0.5	47.4	96.4 ± 30.5	98.7 ± 30.7	88.6

618
 619



620

621 Table 3 Correlations coefficients among diffusive (D_{CH_4} , $mg \cdot m^{-2} \cdot d^{-1}$) and ebullition
 622 (B_{CH_4} , $mg \cdot m^{-2} \cdot d^{-1}$) fluxes observed during individual chamber deployments (576
 623 deployments in total) and environmental variables these variables (water temperatures
 624 (T_w , °C), air temperature (T_a , °C), chlorophyll a concentration ($Chl-a$, $\mu g L^{-1}$), air
 625 pressure (Pa , hPa), the temperature difference between water and air ($\Delta T = T_w -$
 626 T_a , °C)). Correlations are presented for all data and grouped by season.

627

	CH ₄ flux	T _w	T _a	Chl-a	Pa	Δ T	B _{CH₄}
All data	D _{CH₄}	0.492**	0.499**	0.114**	-0.242**	-0.199**	0.224**
	B _{CH₄}	0.372**	0.294**	0.350**	-0.118**	0.042	
Spring	D _{CH₄}	0.679**	0.584**	0.171*	-0.640**	-0.161	0.413**
	B _{CH₄}	0.400**	0.223**	0.125	-0.269**	0.104	
Summer	D _{CH₄}	0.379**	0.319**	-0.446**	-0.246**	-0.053	-0.199*
	B _{CH₄}	-0.194*	-0.258**	0.356**	0.078	0.104	
Autumn	D _{CH₄}	0.844**	0.818**	0.662**	-0.760**	-0.412**	0.527**
	B _{CH₄}	0.577**	0.558**	0.463**	-0.507**	-0.276**	
Winter	D _{CH₄}	0.726**	0.733**	0.024	-0.725**	-0.591**	0.007
	B _{CH₄}	0.133	0.243**	-0.011	-0.141	-0.133	

628

629 **denotes a significant correlation at the 0.01 level; * denotes a significant correlation
 630 at the 0.05 level

631



632 Table 4 Stepwise regressions between diffusive flux of CH₄ (D_{CH_4} , mg·m⁻²·d⁻¹),
 633 and CH₄ ebullition fluxes (B_{CH_4} , mg·m⁻²·d⁻¹), air temperature (T_a , °C), water
 634 temperature (T_w , °C), the temperature difference between water and air ($\Delta T =$
 635 $T_w - T_a$, °C), air pressure (P_a , hPa) and chlorophyll a concentration ($Chl-a$, µg
 636 L⁻¹).

637

Dependent variable	Independent variable	Intercept	Slope	r ²	p
All data					
D_{CH_4}	Ta	0.02	0.004	0.25	<0.001
	Ta + Pa	0.07	0.004 - 0.00005	0.27	<0.001
	Ta + Pa + B_{CH_4}	0.07	0.004 - 0.00005 + 0.001	0.28	<0.001
Spring					
D_{CH_4}	Pa	7.81	-0.008	0.28	<0.001
	Pa + Chl-a	6.87	-0.007 + 0.000	0.43	<0.001
	Pa + Chl-a + T_w	-2.17	0.002 + 0.000 + 0.019	0.52	<0.001
	Chl-a + T_w	-2.45	0.000 + 0.016	0.52	<0.001
Summer					
D_{CH_4}	Chl-a	0.18	0.000	0.20	<0.001
	Chl-a + T_w	0.08	-0.0001 + 0.003	0.23	<0.001
Autumn					
D_{CH_4}	T_w	-0.10	0.007	0.71	<0.001
Winter					
D_{CH_4}	Ta	0.02	0.007	0.54	<0.001
	Ta + Pa	6.05	0.004 - 0.006	0.63	<0.001
	Ta + Pa + B_{CH_4}	6.21	0.004 - 0.006 - 0.003	0.64	<0.001
	Ta + Pa + B_{CH_4} + Chl-a	7.58	0.004 - 0.007 - 0.003 + 0.000	0.65	<0.001

638

639



640

641 Table 5 Stepwise regressions between CH₄ ebullition fluxes (B_{CH_4} , mg·m⁻²·d⁻¹) and
 642 diffusive flux of CH₄ (D_{CH_4} , mg·m⁻²·d⁻¹), air temperature (T_a , °C), water temperature
 643 (T_w , °C), the temperature difference between water and air ($\Delta T = T_w - T_a$, °C), air
 644 pressure (P_a , hPa) and chlorophyll a concentration ($Chl-a$, µg L⁻¹).

645

Dependent variable	Independent variable	Intercept	Slope	r ²	p
All data					
B_{CH_4}	T_w	-3.80	0.39	0.14	<0.001
	$T_w + chl-a$	-4.28	0.292 + 0.011	0.19	<0.001
	$T_w + chl-a + \Delta T$	-4.99	0.315 + 0.010 + 0.188	0.20	<0.001
	$T_w + chl-a + \Delta T + D_{CH_4}$	-5.04	0.271 + 0.010 + 0.206 + 8.687	0.20	<0.001
Spring					
B_{CH_4}	D_{CH_4}	-1.62	40.67	0.17	<0.001
	$D_{CH_4} + \Delta T$	-2.98	43.45 + 0.411	0.20	<0.001
	$D_{CH_4} + \Delta T + T_a$	-16.29	15.78 + 1.406 + 0.787	0.26	<0.001
	$\Delta T + T_a$	-19.56	1.695 + 1.038	0.25	0.027
	$\Delta T + T_a + P_a$	-502.71	2.74 + 1.998 + 0.459	0.32	0.013
Summer					
B_{CH_4}	$Chl-a$	2.59	0.02	0.13	<0.001
Autumn					
B_{CH_4}	T_w	-13.73	0.807	0.33	<0.001
Winter					
B_{CH_4}	$Chl-a$	2.53	-0.01	0.04	0.015

646



647 Table 6 Correlation coefficients between daily total diffusive CH₄ flux (T_{DCH_4} ,
 648 mg·m⁻²·d⁻¹), daily total CH₄ ebullition (T_{BCH_4} , mg·m⁻²·d⁻¹), the frequency of daily
 649 CH₄ ebullition (F_{BCH_4} , %) and mean daily environmental variables (Daily mean
 650 air temperature ($\overline{T_a}$, °C), daily mean water temperatures ($\overline{T_w}$, °C), daily mean air
 651 pressure ($\overline{P_a}$, hPa), daily mean chlorophyll a ($\overline{chl-a}$, µg L⁻¹), daily mean
 652 concentrations of total nitrogen (\overline{TN} , mg L⁻¹) and daily mean concentrations of
 653 total phosphorus (\overline{TP} , mg L⁻¹)).

654
 655

Variable	$\overline{T_w}$	$\overline{T_a}$	$\overline{chl-a}$	$\overline{P_a}$	\overline{TN}	\overline{TP}	F_{BCH_4}	T_{BCH_4}
T_{DCH_4}	0.568 (0.054)	0.537 (0.072)	0.208 (0.517)	-0.510 (0.091)	-0.499 (0.118)	-0.494 (0.123)	0.551 (0.063)	0.538 (0.071)
T_{BCH_4}	0.703** (0.011)	0.684** (0.014)	0.660* (0.02)	-0.650* (0.022)	0.008 (0.982)	-0.054 (0.874)	0.932** (0.000)	
F_{BCH_4}	0.738** (0.006)	0.735** (0.007)	0.579** (0.048)	-0.635* (0.026)	0.086 (0.802)	0.083 (0.808)		

656

657 **denotes a significant correlation at the 0.01 level; * denotes a significant correlation
 658 at the 0.05 level

659



660 Table 7 Parameters of regression models (used in supplement Fig.1) of diffusive and
 661 ebullitive CH₄ fluxes as a function of water temperatures (*T_w*) at different
 662 concentrations of total phosphorous (*TP*).
 663
 664
 665

Emissions (mg·m ⁻² ·h ⁻¹)	Averaged TP (mg·L ⁻¹)	n	T _w			T _a		
			Q ₁₀	p	R ²	Q ₁₀	p	R ²
CH ₄ diffusive	0.05	144	1.29	<0.001	0.26	1.27	<0.001	0.36
	0.1	96	1.79	<0.001	0.46	1.62	<0.001	0.58
	0.2	48	5.29	0.002	0.23	1.86	<0.001	0.29
	0.4	144	7.52	<0.001	0.69	5.23	<0.001	0.43
	0.8	96	5.24	<0.001	0.76	3.24	<0.001	0.71
CH ₄ ebullition	0.05	51	1.32	0.046	0.08	1.15	0.192	0.02
	0.1	52	1.85	0.211	0.04	1.27	0.407	0.02
	0.2	--	--	--	--	--	--	--
	0.4	--	--	--	--	--	--	--
	0.8	53	3.29	<0.001	0.21	2.06	0.001	0.17

666
 667
 668
 669

-- indicates that no exponential relationships were found



670 Figure Captions

671

672 Fig. 1 Diurnal and seasonal variability of the main environmental factors and
673 CH₄ fluxes during the monitoring periods.

674

675 Fig. 2 Bin-averaged diffusive CH₄ flux (D_{CH_4}) and the difference between water and
676 air temperature ($\Delta T = T_w - T_a$). Symbols showed mean values within each
677 temperature bin, error bars showed the respective standard deviation (SD represented
678 the degree to which the data value deviates from the mean). The ellipse of the dotted
679 line indicated D_{CH_4} when ΔT was close zero.

680

681 Fig. 3 Changes of CH₄ ebullition (B_{CH_4} , histograms) and frequency of daily CH₄
682 bubbling (grey area) versus the temperature difference between water and air (Δ
683 T).

684

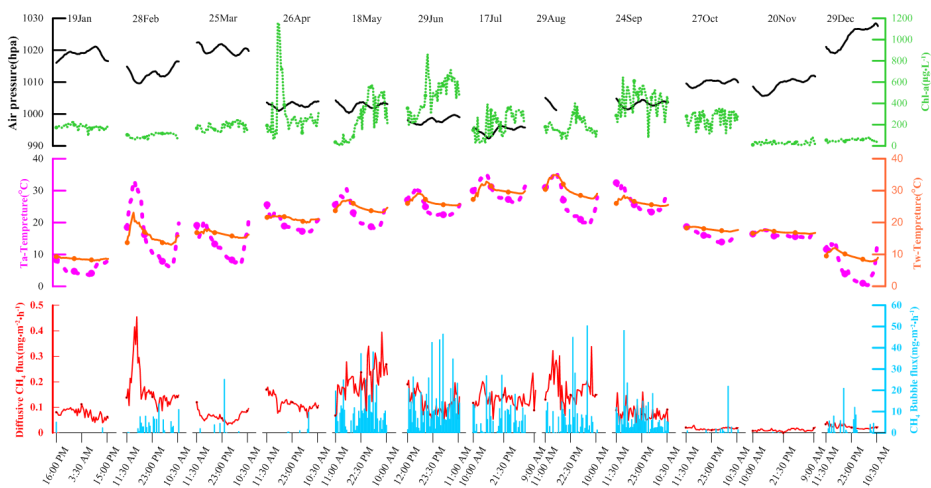
685 Fig. 4 (a) Daily total diffusive CH₄ flux (T_{DCH_4}), and (b) daily total CH₄ ebullition (T_{BCH_4})
686 as a function of mean daily water temperature ($\overline{T_w}$, black circles) and air temperature
687 ($\overline{T_a}$, open circles). The solid lines represent the exponential relationships between pond
688 fluxes and $\overline{T_w}$, the dashed lines represent the exponential relationships between pond
689 fluxes and $\overline{T_a}$. The values of the temperature coefficient Q_{10} and the coefficients of
690 determination (R^2) for the exponential fits are provided as labels in each graph.

691



692 Fig. 1 Diurnal and seasonal variability of the main environmental factors and CH₄
693 fluxes during the monitoring periods.

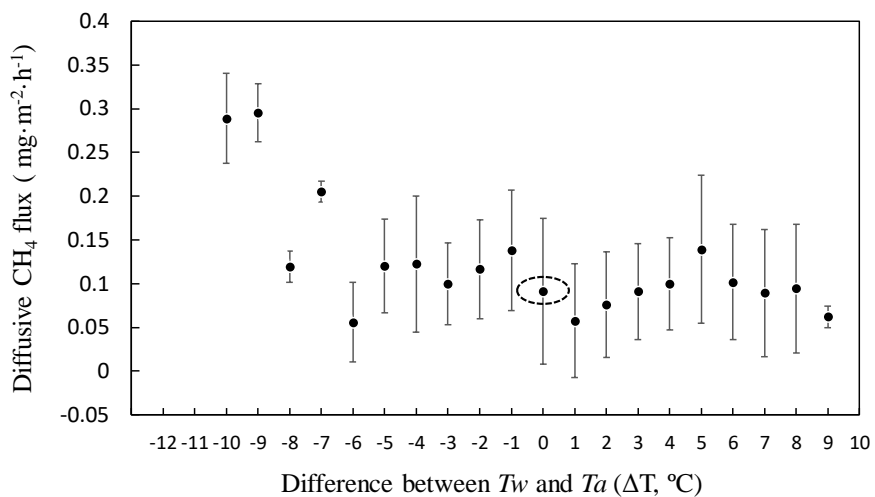
694
695
696
697



698
699
700
701
702



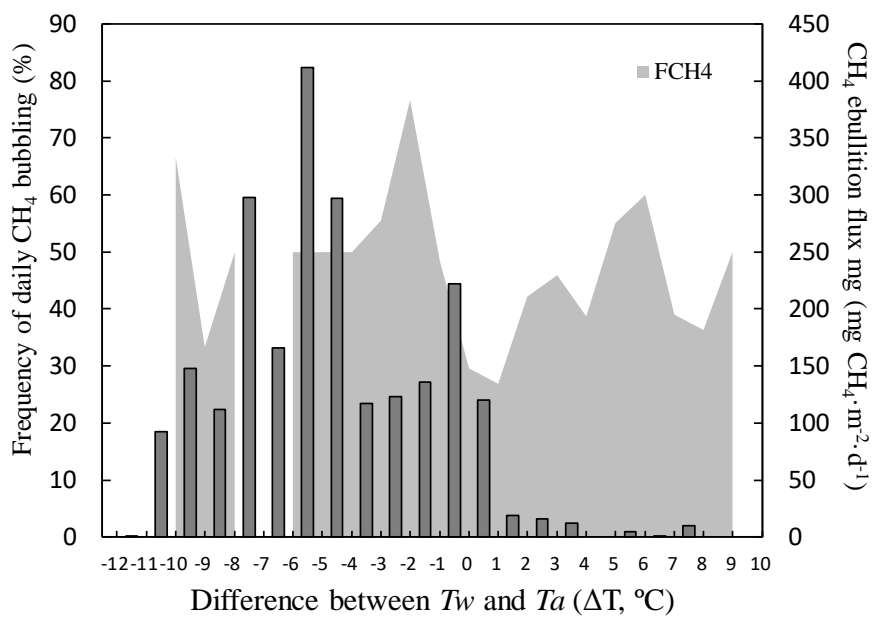
703 Fig. 2 Bin-averaged diffusive CH_4 flux (D_{CH_4}) and the difference between water and air
704 temperature ($\Delta T = T_w - T_a$). Symbols showed mean values within each temperature bin,
705 error bars showed the respective standard deviation (SD represented the degree to which the
706 data value deviates from the mean). The ellipse of the dotted line indicated D_{CH_4} when ΔT
707 was close zero.



716



717 Fig. 3 Changes of CH_4 ebullition (B_{CH_4} , histograms) and frequency of daily CH_4 bubbling (grey
718 area) versus the temperature difference between water and air (ΔT).
719
720





732 Fig. 4 (a) Daily total diffusive CH_4 flux (T_{DCH_4}), and (b) daily total CH_4 ebullition (T_{BCH_4}) as a
733 function of mean daily water temperature ($\overline{T_w}$, black circles) and air temperature ($\overline{T_a}$, open
734 circles). The solid lines represent the exponential relationships between pond fluxes and $\overline{T_w}$,
735 the dashed lines represent the exponential relationships between pond fluxes and $\overline{T_a}$. The
736 values of the temperature coefficient Q_{10} and the coefficients of determination (R^2) for the
737 exponential fits are provided as labels in each graph.
738

739

